Seal Analysis for the Ares-I Upper Stage Fuel Tank Manhole Covers

Dawn R. Phillips[1] and Robert J. Wingate[2]
Dynamics, Loads, and Strength Branch, NASA Marshall Space Flight Center, Huntsville, Alabama, 35812

Techniques for studying the performance of Naflex pressure-assisted seals in the Ares-I Upper Stage liquid hydrogen tank manhole cover seal joint are explored. To assess the feasibility of using the identical seal design for the Upper Stage as was used for the Space Shuttle External Tank manhole covers, a preliminary seal deflection analysis using the ABAQUS commercial finite element software is employed. The ABAQUS analyses are performed using three-dimensional symmetric wedge finite element models. This analysis technique is validated by first modeling a heritage External Tank liquid hydrogen tank manhole cover joint and correlating the results to heritage test data. Once the technique is validated, the Upper Stage configuration is modeled. The Upper Stage analyses are performed at 1.4 times the expected pressure to comply with the Constellation Program factor of safety requirement on joint separation. Results from the analyses performed with the External Tank and Upper Stage models demonstrate the effects of several modeling assumptions on the seal deflection. The analyses for Upper Stage show that the integrity of the seal is successfully maintained.

I. Introduction

THE objective of this paper is to perform analyses of the Ares-I US LH2 tank manhole cover seal joint to predict relative deflections between the cover and the LH2 tank dome-cover flange to assess the feasibility that the Naflex seal used with the ET manhole covers can successfully be used for the Ares-I design. Ares-I is the two-stage crew launch vehicle for NASA's Constellation Program. Ares-I consists of a solid-fueled first stage, and a liquid-fueled Upper Stage (US) that uses liquid hydrogen (LH2) and liquid oxygen (LOX) to power a single J-2X engine.

The insulated US structure includes two tanks to hold the LH2 and LOX at cryogenic temperatures. The design of the domes includes "manholes" to provide access to the inside of the tanks. During final assembly, covers will be placed over these manholes. To prevent leaking of the liquid propellant or ullage gas when the tanks are filled, seals will be placed between the manholes and the covers.

In the Saturn and Space Shuttle Programs, Naflex seals were used to seal the joints between the manholes and the covers in the propellant tanks. In this paper, a preliminary assessment is presented of the feasibility of using the Space Shuttle External Tank (ET) manhole cover Naflex seal design in the Ares-I US manhole cover joints. As part of the assessment, a seal analysis technique different from that used by the ET Project is explored.

Naflex seals are spacer-type, deflection-activated, pressure-assisted, static seals. The seal configuration uses a cantilevered, deflection-loaded primary seal and a simple gasket-type secondary seal. A cross-sectional view of the seal is shown in Figure 1(b). The cantilevered beams or legs form a fork on the pressure side of the seal. In the uninstalled configuration, the tips of the cantilevered legs protrude beyond the rest of the seal in the X direction (see Figure 1(b)). The seal is installed in the joint between two flat flanges, and during joint assembly, when the bolts are preloaded, deflection of the legs provides the initial contact load to accomplish sealing at the primary seal-flange interface, creating the primary sealing surface. Pressurization of the joint forces the legs even tighter against the sealing surface (Anon, undated; Anon, ca. 2000; Anon., 2001; and Robbins and Ludtke, 1964). In addition, the area around the bolt hole provides a secondary sealing surface as it is also placed in compression due to the bolt preload. Naflex seals are commonly fabricated of Inconel 718 with a Teflon enamel coating. The manhole cover seal design used by the ET Project has a heritage traceable to the Saturn S-II stage. The Naflex seal under consideration in this paper is shown in Figure 1. The seal has a 92-hole bolt circle around the circumference.

[1] Aerospace Engineer, Senior Member, AIAA.
[2] Aerospace Engineer and Team Lead.

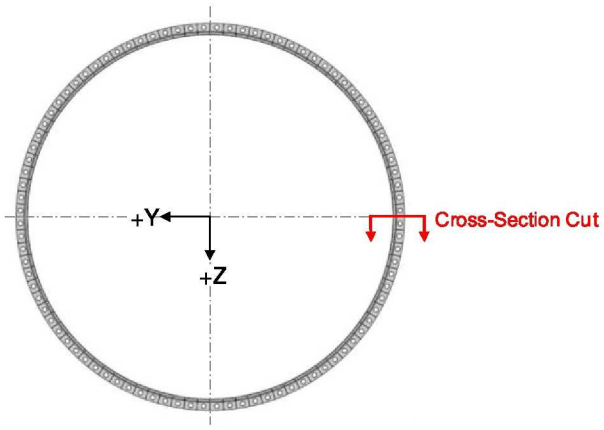

(a) Top view

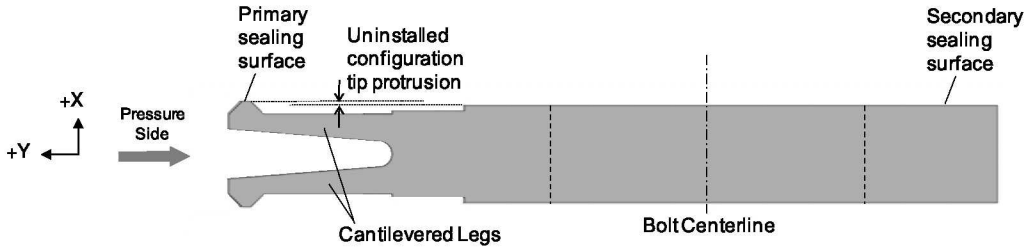

(b) Cross-sectional view

Figure 1. Naflex seal.

The paper is organized as follows. First, analytical background of the axisymmetric analysis technique and test-verification program employed by the ET Project is provided. Next, the analyses performed for this paper are described. Three-dimensional finite element models for the ET LH2 tank manhole cover seal are correlated with the heritage ET seal test results. Then, the modeling practices established by the ET analyses are used to construct models for the Ares-I US LH2 tank manhole cover, and the seal deflection analyses are presented.

II. Analytical Background

The sealing performance of the ET Naflex seals was originally qualified by similarity (Anon., 1976), presumably to heritage Saturn-era seals. Subsequent computer simulations of the manhole cover joints for both the LH2 and LOX tanks of the ET were performed during the 1980s (most recently, Pilet and Geiman, 1997) using BOSOR5 (Bushnell, 1974 and 1976). BOSOR5 is a finite difference energy minimization code that performs large-deflection axisymmetric stress analysis, small-deflection nonsymmetric stress analysis, and buckling analysis. For an applied pressure loading, relative deflections between specified nodes that represented the seal, the tank dome (the manhole), and the manhole cover were computed. These deflections were compared to the seal deflection limits levied in the Saturn-era seal design specification. This specification on seal deflection requires that the primary seal not leak unacceptably at established temperature and pressure conditions and with a total joint axial deflection (joint opening) of Δ_{spec}. Furthermore, this specification is usually interpreted as a one-sided seal deflection such that each flange of the joint opens no more than $\Delta_{spec}/2$. The worst-case deflection predicted by the ET analyses was at the ET LH2 aft manhole cover joint and exceeded Δ_{spec}. A test program was then conducted to validate the BOSOR5 models and also to determine the maximum seal deflection that can be present before sealing capability is lost.

The test program verified the sealing capability of the seals for the ET tank configurations, temperatures, and pressures, and the BOSOR5 analysis models were correlated to the test results (Gillespie, 1988). The design specification for seal deflection was determined to be overly conservative, and a new seal deflection allowable for the ET joint configuration Δ_{ET} was derived.

All subsequent analyses of seal deflection under ET flight loads conducted by the ET Project continued to use the BOSOR5 modeling technique with the derived seal deflection allowable Δ_{ET} as the success criterion.

III. Analysis

Seal deflection analysis of the US LH2 tank manhole cover seal joint initially attempted to use the same BOSOR5 axisymmetric modeling technique employed by the ET Project because the US LH2 tank manhole cover design is similar to that of the ET, and the ET Naflex seal models had been anchored to test data.

However, after attempting this analysis, it became apparent that a different modeling technique was necessary because

- The ET manhole cover BOSOR5 models were created and run in an older, customized version of BOSOR5 that is no longer supported nor compatible with newer versions.
- Newer versions of BOSOR5 may not provide the most efficient method for this type of analysis due to the axisymmetric simplifications of the bolted joint.

Therefore, three-dimensional (3D), symmetric wedge finite element (FE) analyses are performed using the ABAQUS[3] commercial FE software. All of the analyses presented in this paper are nonlinear analyses. The bolt preload is applied during the first step of the analysis, and then the pressure load is applied during a second, subsequent step.

The 3D FE analysis technique has several perceived benefits.

- The LH2 tank dome and manhole cover designs of the ET and US are similar but not exactly the same; a new FE model built uniquely for US allows the behavior of the LH2 tank manhole cover joint to be better understood.
- The design of the LOX tank cover on US is significantly different from ET, requiring new models to eventually be created.
- A three-dimensional analysis methodology allows some of the assumptions associated with the axisymmetric modeling to be relaxed and the features of the seal joint to be modeled explicitly. Because more features of the seal joint can be modeled explicitly, more options are available for interrogating the analysis results and assessing the performance of the seal.

A. 3D Finite Element Seal Joint Analyses

As a first step in a methodical approach to the analysis, symmetric wedge models for the ET LH2 tank manhole cover seal joints are correlated with the ET seal test results (see Gillespie, 1988). The 3D FE modeling practices established with the ET models are then used to construct an Ares-I US LH2 tank model to assess the manhole cover (MHC) seal performance under flight environments.

1. ET Seal Test-Analysis Correlation

a. ET Seal Test

The ET seal test was designed partly to demonstrate the ability of the BOSOR5 models to predict measured seal deflections. Because the worst-case seal deflection predicted by the BOSOR5 analyses was at the LH2 tank aft manhole cover joint, the ET seal test utilized a flight-ready LH2 tank aft MHC. A simplified view of the ET LH2 tank aft MHC is shown in Figure 2. This MHC and a flight-quality Naflex seal were mounted to a rigid fixture tool as depicted in Figure 3. The test was conducted at room temperature.

The test article was pressurized in 25-percent increments up to a specified target pressure. At each pressure increment, the vertical defection of the MHC was measured at five locations, D1, D2, D3, D4, and D5, as shown in Figure 4(a). Locations D1, D3, and D5 are each in line with a bolt, while locations D2 and D4 are between bolts. The deflection was measured, as shown in Figure 4(b), on the top surface of the MHC at the radius corresponding to the seal primary sealing surface, R_{PSS}. It was assumed that no relative motion occurred between the outer and inner surfaces of the MHC; the rigid fixture was assumed to not deform, and all of the vertical deflection was due to translation of the MHC. Therefore, the measured vertical deflection on the outside of the cover was assumed to be an accurate measure of the seal deflection. The finite element analyses performed for this paper validate this assumption, and hence, for convenience in presentation, the results will be presented as seal deflections.

The seal deflections vs. pressure for the ET test are shown in Figure 5. In Figure 5, the normalized seal deflections at each of the locations D1-D5 and the average seal deflection for all of the locations are plotted. The seal deflections are normalized by the average seal deflection at the target pressure.

[3] ABAQUS is a registered trademark of Dassault Systèmes.

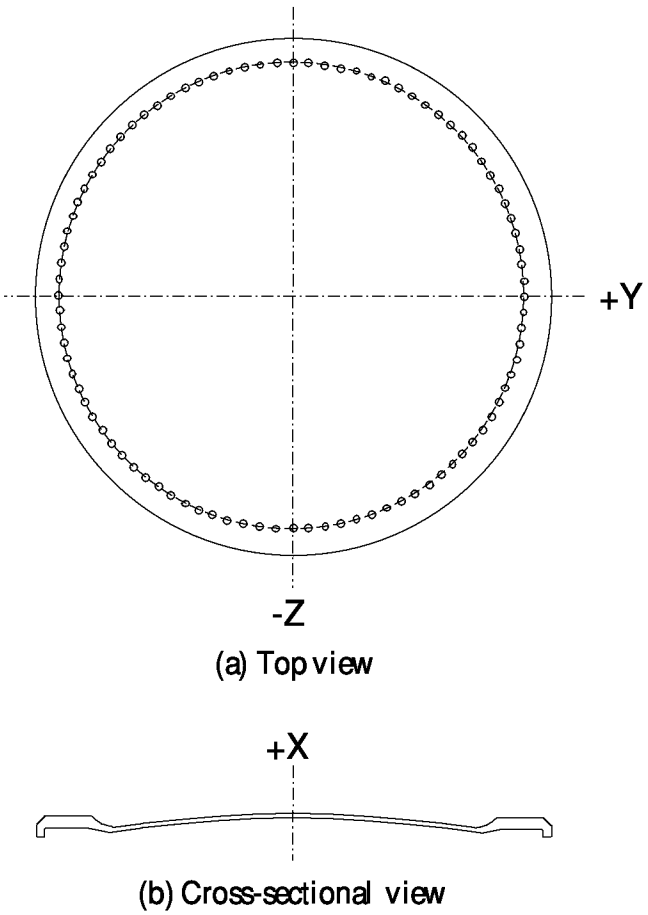

Figure 2. Simplified view of ET LH2 tank aft MHC.

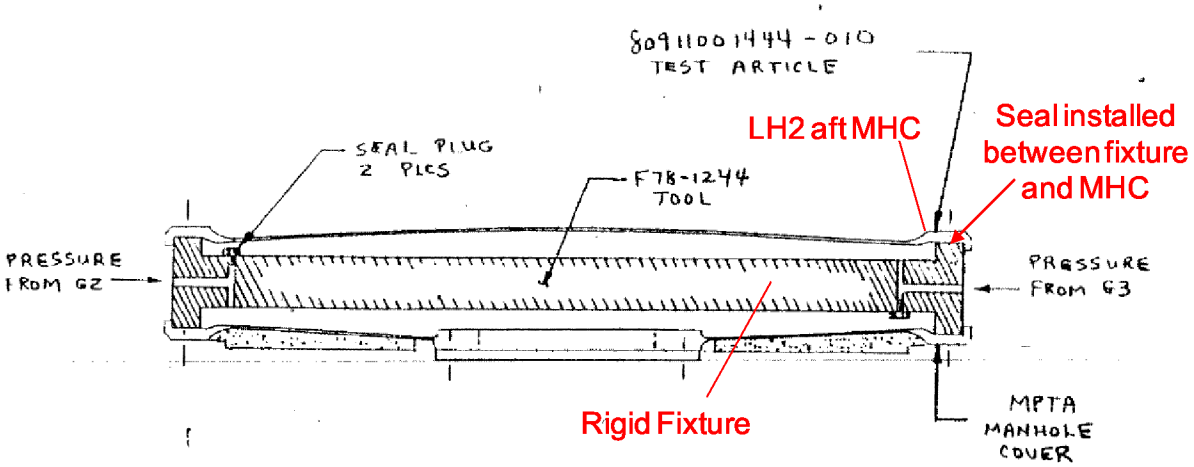

Figure 3. Cross-sectional view of ET LH2 tank aft MHC test set-up (drawing from Gillespie, 1988).

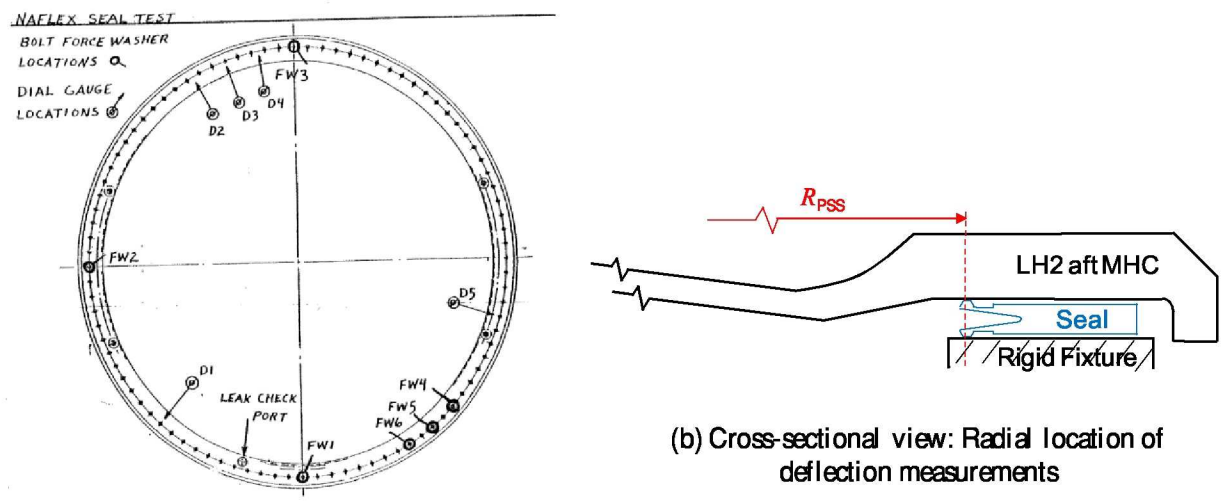

(a) Top view: Gauge locations around the MHC (drawing from Gillespie, 1988)

(b) Cross-sectional view: Radial location of deflection measurements

Figure 4. Locations of vertical deflection measurement during ET seal test.

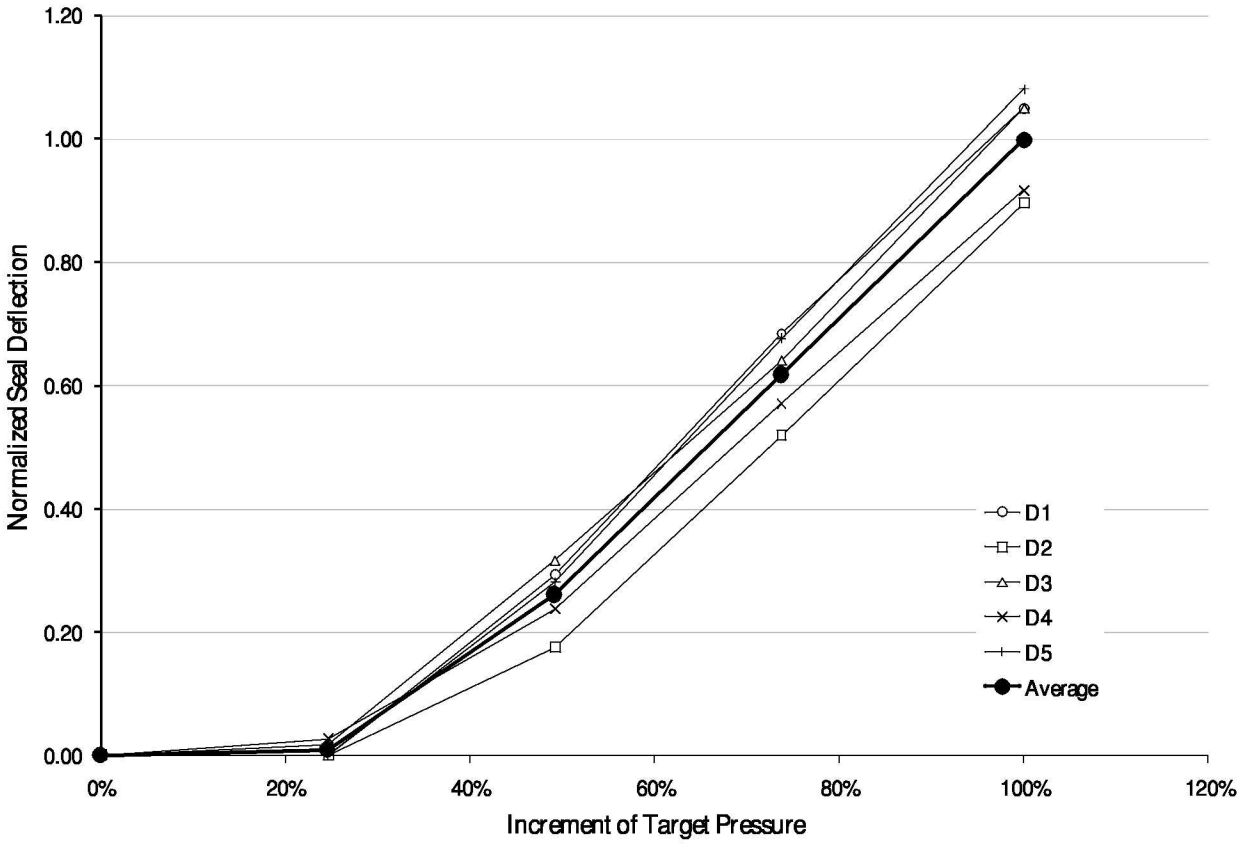

Figure 5. Seal deflections for the ET seal test.

b. 3D Finite Element Model

A 3D solid FE model of the ET LH2 tank aft MHC is created by exploiting the near symmetry of the MHC. A wedge section of the MHC that encompasses a single bolt, or 3.913°, as shown in Figure 6(a), is used. A close-up of the symmetric wedge FE model is shown in Figure 6(b). The local region around the bolt hole is modeled with 3D solid elements, and the region away from the bolt hole is modeled with shell elements. The two regions are joined using a shell-to-solid coupling constraint for smooth transition of loads across the shell/solid interface. This practice enables the use of shell theory, which is appropriate for the tank configurations, in conjunction with solid modeling, which is required to capture greater detail at the seal joint.

Similarly, a 3.913° wedge FE model of the Naflex seal is created. This model is shown in Figure 7. The seal is modeled entirely with solid elements. The Teflon coating is not explicitly modeled; rather, the effects are modeled using a coefficient of friction in the seal contact definition, which is discussed later.

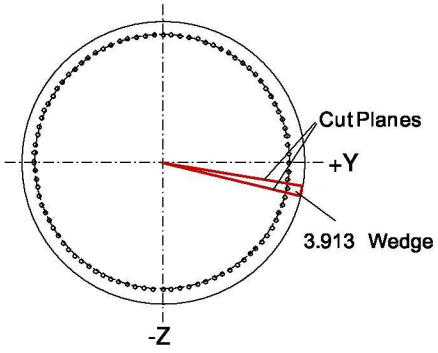

(a) Symmetric wedge of aft MHC

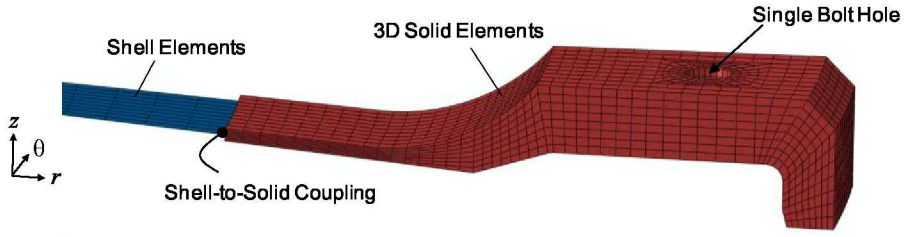

(b) Close-up view of 3.913° wedge finite element model with local cylindrical coordinate system

Figure 6. Symmetric wedge of ET LH2 tank aft MHC.

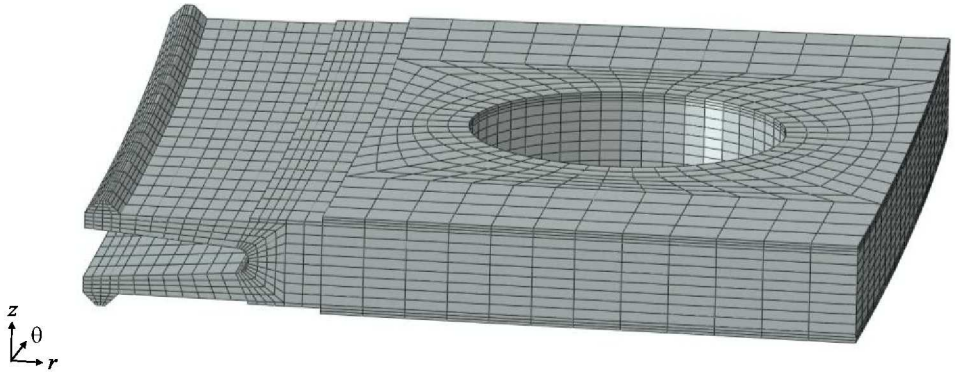

Figure 7. Finite element model of 3.913° wedge of Naflex seal.

The FE model of the ET test set-up is shown in Figure 8. The model consists of three main parts: the MHC incorporating both shell and solid modeling, the seal, and a 3.913° wedge to represent the rigid fixture. Because the test fixture is assumed to be rigid, the bottom surface of the fixture model is fixed (i.e., $u_r = u_\theta = u_z = 0$). Symmetric boundary conditions (i.e., $u_\theta = 0$) are applied to the $\theta = 0$ and $\theta = 3.913°$ cut planes. The preload is applied to the bolt during the first analysis step. The pressure is applied along the inside surface of the MHC and around the pressure side of the seal legs, as shown in Figure 8, during the second analysis step. Contact is defined between the seal and the MHC and between the seal and the fixture. More details of the contact modeling in these two regions will be presented later. In addition, contact is defined between the lip of the MHC and the outer surface of the fixture (see Figure 8).

The modeling of the bolted joint is achieved by the use of beam elements to represent the bolt and "spider" constraints to represent the interaction of the bolt with the connected parts. An example of the bolted joints in the ET MHCs is shown in Figure 9(a). These joints consist of a bolt, a corresponding threaded insert, and a washer. The representation of the bolted joint in the FE models is shown in Figures 9(b-c). The bolt preload is applied using the ABAQUS bolt load capability: a pretension section is defined on the bolt, the preload is applied as a force to the pretension section, and then the bolt length is fixed. On the MHC side, the spider constraint couples the displacements of the chosen nodes on the outer surface, representing the size of the washer bearing surface (see Figure 9(b)), to the motion of a single node corresponding to the bolt head. On the fixture side, the spider constraint couples the displacements of the chosen nodes on the inside surface of the threaded insert hole (see Figure 9(c)) to a single node corresponding to the bolt end, representing the bolt-engagement BC.

The solid elements are the ABAQUS C3D8I elements, which are 8-node brick elements with additional internal freedoms introduced as incompatible modes for improved bending behavior[4]. In general, in the MHC, there are eight brick elements for every half inch of thickness. The shell elements are the ABAQUS S4 elements, which are 4-node quadrilateral elements, and the beam elements are the ABAQUS B31 elements, which are 2-node Timoshenko beam elements. Overall, the test set-up FE model contains 16208 elements: 8 beam elements, 488 shell elements, and 15712 brick elements.

Linear, elastic material properties are assumed for all of the materials. The materials used for the current analyses are provided in Table 1. To simulate the rigid test fixture, the modulus is arbitrarily set three orders of magnitude higher than the moduli for the other materials.

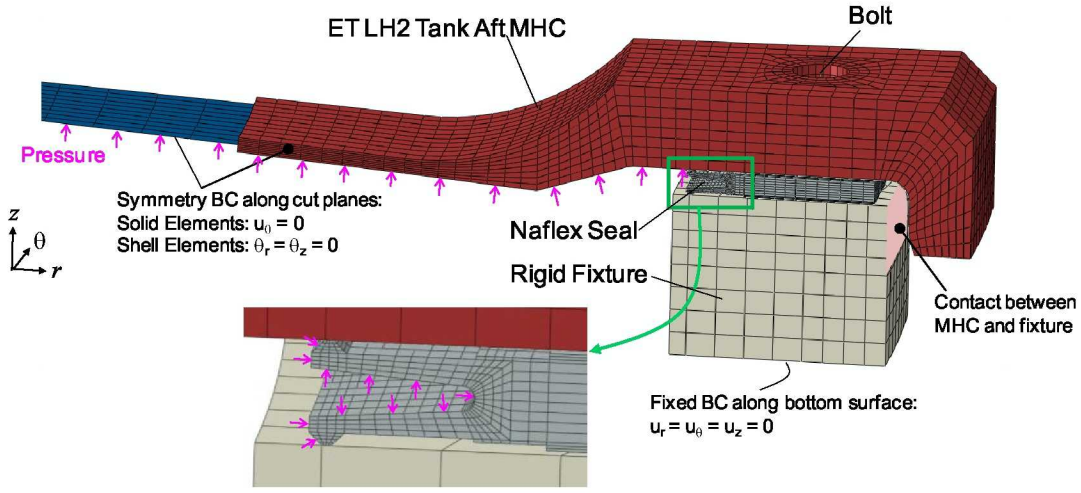

Figure 8. Finite element model of test set-up.

[4] The C3D8I solid element has 8 nodes with three degrees of freedom per node plus 13 additional element variables associated with the incompatible deformation modes. The estimated total number of unknowns for a given finite element mesh using C3D8I elements is roughly equal to three times the number of nodes plus 13 times the number of C3D8I solid elements.

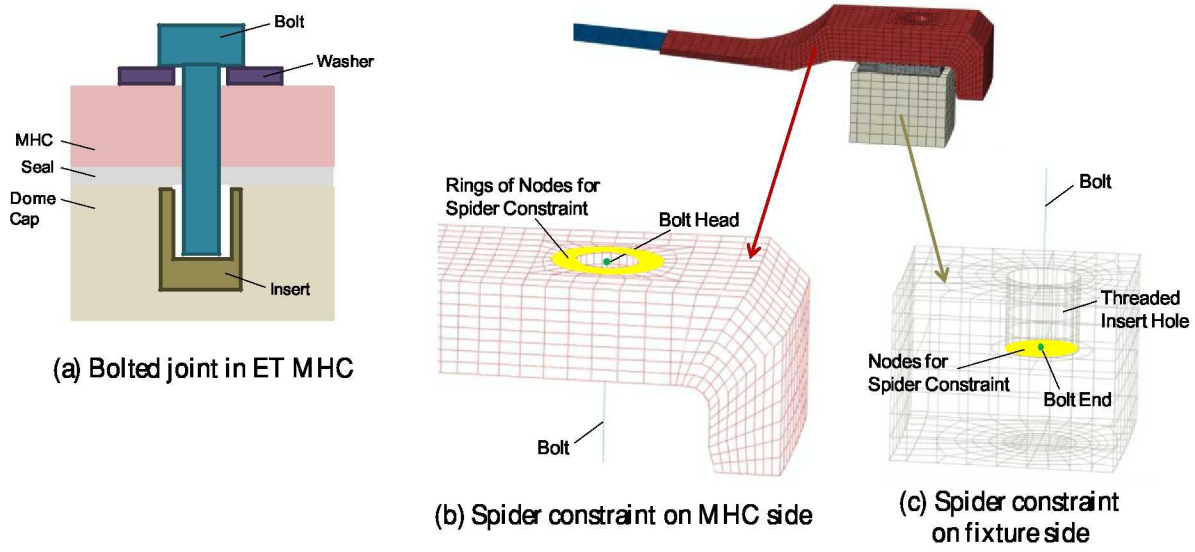

(a) Bolted joint in ET MHC

(b) Spider constraint on MHC side

(c) Spider constraint on fixture side

Figure 9. The bolted joint.

Table 1. Linear, elastic material properties for the ET seal test set-up FE analyses.

Part	Material	E, psi @ RT	ν @ RT
MHC	Aluminum 2219	10.5×10^6	0.33
Seal	Inconel 718	30×10^6	0.3
Bolt	A286 Stainless Steel	30×10^6	0.29
Fixture	n/a	10×10^9	0

The modeling of the contact between the seal and the MHC and between the seal and the fixture requires special handling. As discussed previously, the fixed boundary condition (which removes the rigid body modes from the problem) is applied to the bottom of the fixture, and the MHC is connected to the fixture via the bolt modeling and spider constraints. However, the seal, which sits between the MHC and the fixture, is an unconnected region; i.e., it is not physically connected to either the MHC or the seal, and hence could cause numerical singularities. A cross-sectional view of the seal contact surfaces is shown in Figure 10. In the figure, initial contact at the primary sealing surface (PSS) and an initial gap at the secondary sealing surface (SSS) are shown. Note that the surface area of the SSS is much greater than the surface area of the PSS. When modeling contact in ABAQUS, any surfaces that are in initial contact with each other allow the corresponding nodal entries in the global stiffness matrix to be populated during the initial set-up (the zeroth solution increment), thus reducing the chance for numerical singularities to occur. In order to take advantage of this, two separate contact interactions are defined for the PSS and the SSS.

For both contact interactions, a finite-sliding, surface-to-surface formulation is used. The finite-sliding formulation utilizes the true representation (rather than a linear approximation) of the master surface for the slave surface interaction. The surface-to-surface formulation enforces contact in an average sense over the slave surface, rather than enforcing contact at the individual nodes on the slave surface. Finite-sliding and surface-to-surface are the most general contact formulations available in ABAQUS, and they tend to yield better solutions for a wide range of problems than the other formulations (Anon, 2009). The constraint enforcement method in the direction normal to the contact surfaces is defined as "Hard" contact. In Hard contact, zero clearance between the contact surfaces is strictly enforced whenever contact pressure is detected. The constraint enforcement method in the direction tangential to the contact surfaces uses a penalty formulation. Because the seal is not physically connected to the other regions of the model, frictionless contact causes numerical difficulties, and a converged solution cannot be obtained. Therefore, a coefficient of friction is assigned for contact in the tangential direction. The use of a coefficient of friction, while not necessarily conservative, is not unreasonable in these problems because the Teflon coating on the seal provides some resistance to sliding.

For the contact interactions between the seal and the MHC, the master surface is defined as the bottom surface of the MHC, as highlighted by the green line in Figure 10. For the PSS, the slave surface is defined as the top surface of the seal tip, as indicated by the yellow line in Figure 10. To ensure that the two surfaces are recognized as being

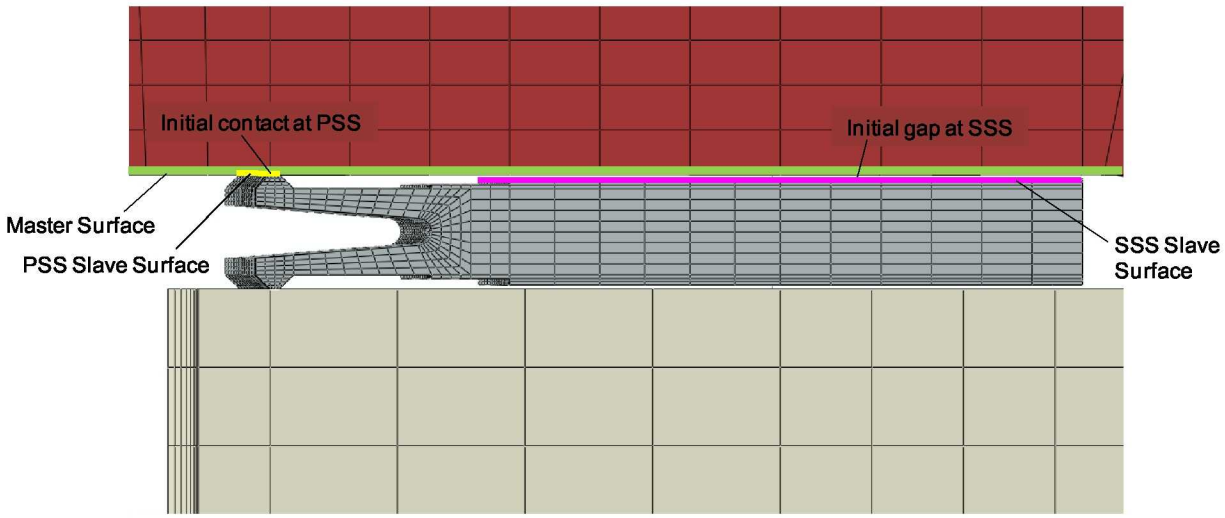

Figure 10. Seal contact surfaces.

in initial contact, and hence populate the global stiffness matrix, the ABAQUS option to adjust the slave node initial positions is used. For the SSS, the slave surface is defined as the top surface of the seal, as indicated by the magenta line in Figure 10. To maintain the initial gap, the slave node initial positions are not adjusted. Identical contact interactions are defined between the seal and the fixture.

Initial analyses performed for this model did not converge. Because the surface-to-surface formulation enforces contact in an average sense over the slave surface, it generates unsymmetric terms in the global stiffness matrix. Therefore, the use of the unsymmetric matrix storage and solver was required to obtain converged solutions.

c. Results

The baseline FE model of the ET seal test set-up, hereafter referred to as the Baseline-ET model, is shown in Figure 8 and is characterized by the following:

- The bolt preload is the preload used in the ET test.
- The pressure load is the target pressure from the ET test.
- The ring of nodes for the spider constraint on the MHC encompasses two rings of elements, as shown in Figure 9(b), thus modeling a bearing surface defined by the washer outer diameter.
- The nodes for the spider constraint on the fixture include all of the nodes on the bottom surface of the threaded insert hole, as shown in Figure 9(c).
- The coefficient of friction for the contact between the seal and the MHC and between the seal and the fixture is $\mu = 0.1$.
- The contact between the MHC and the fixture (see Figure 8) is frictionless; i.e., $\mu = 0$.

The seal deflection from the analysis results is computed by subtracting the seal gap (see Figure 11) at the end of the preload step from the seal gap at the end of the pressure step, or

$$\Delta_z = \delta_z^{\text{pressure}} - \delta_z^{\text{preload}} \tag{1}$$

The seal deflection is computed at two locations: directly in line with the center of the bolt hole and exactly between two bolt holes (i.e., a node on the plane of symmetry). Then the values from the two locations are averaged.

The results for Δ_z vs. pressure for the Baseline-ET model are compared to the average seal deflections from the ET test in Figure 12. As expected, the slope of the curve for the Baseline-ET model results is nearly linear. This is in contrast to the test results, which show nearly zero deflection up to 25 percent of the target pressure and then a linear response up to the target pressure. The reason for this bilinear response is hypothesized to be due to stiction and load redistribution sometimes observed on the initial application of load to structural assemblies. The test report (Gillespie, 1988) indicates that the pressure was simply applied in 25-percent increments up to the target pressure and that deflection readings were taken (as discussed previously) at each increment. However, had the test procedure required applying only the first and second increments of pressure, then unloading the test specimen and re-zeroing the instrumentation, followed by applying the pressure increments to the final target pressure, it is

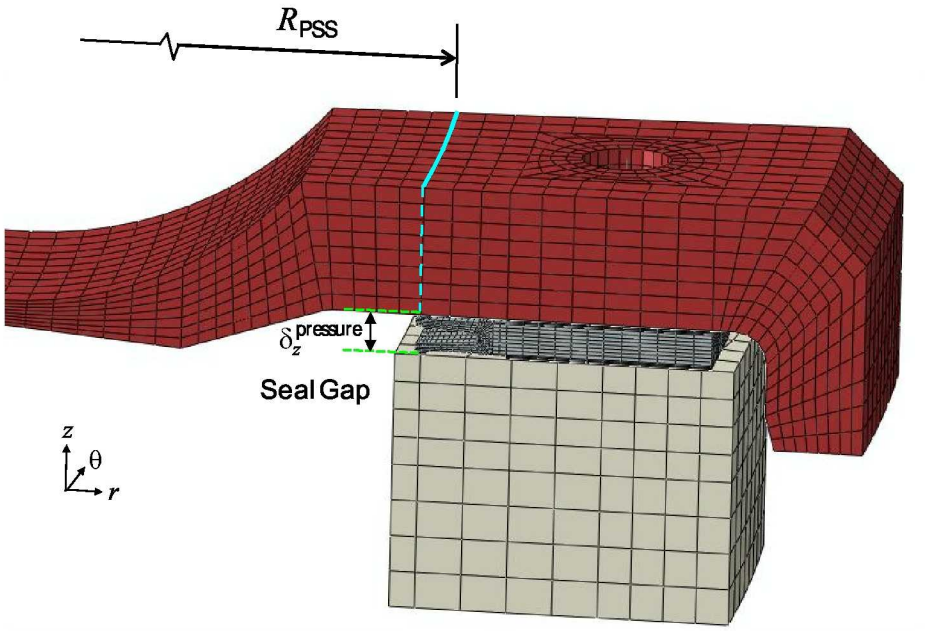

Figure 11. Seal gap $\delta_z^{pressure}$ due to the pressure load.

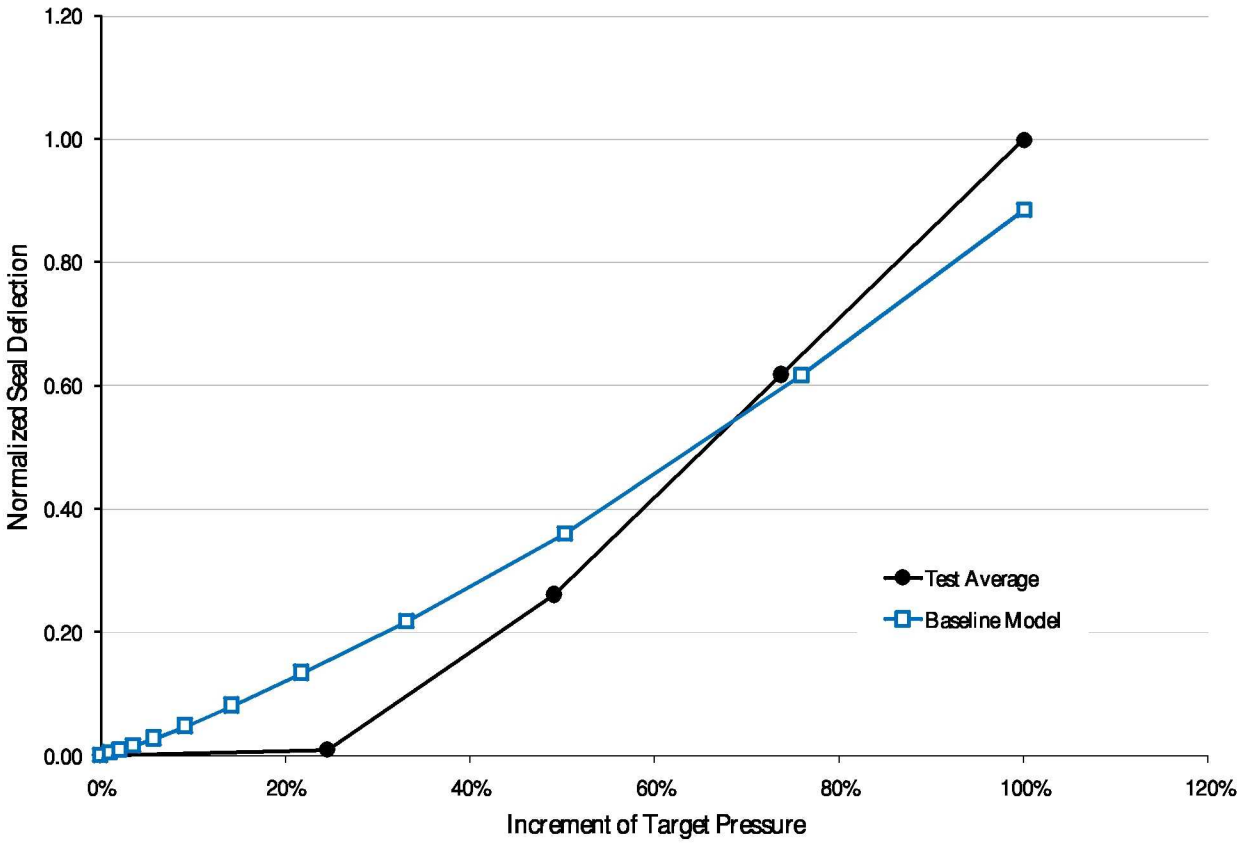

Figure 12. Comparison between test and baseline analysis results for seal deflection vs. pressure.

possible that a more linear deflection response would have been observed. However, this hypothesis cannot truly be verified unless a new test is performed. So while the slope of the predicted seal deflections does not match the test results, seal deflection values at the target pressure can be used to correlate the 3D analysis models to the ET test results.

For the target pressure, the 3D ABAQUS analysis predicts a relative vertical deflection that is eleven percent different from the ET test result. Next, parametric studies are performed to determine the effects of three aspects of the FE modeling on the analysis results and establish better correlation to the test result. These parametric studies include

- Effect of washer-bearing-surface size
- Effect of bolt-engagement BC
- Effect of coefficient of friction

Washer-bearing-surface size. As shown in Figure 9(b), the spider constraint on the MHC connects the node that represents the bolt head to specified nodes on the outer surface of the MHC that represent the size of the washer bearing surface. In the FE model, there are two rings of elements around the bolt hole. The outer ring has a diameter that is equal to the dimension of the washer's outer diameter. In the Baseline-ET model, both rings of elements are used, as shown in Figure 13, representing the entire washer bearing down on the MHC when the bolt preload is applied. Two additional cases (see Figure 13) are also considered: (W1) the inner ring of elements is used for the spider constraint, and (W2) no rings of elements are used; i.e., the ring of nodes on the edge of the bolt hole is used for the spider constraint.

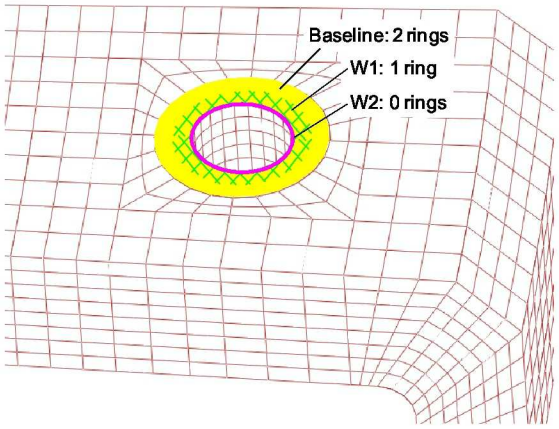

Figure 13. Cases considered to study the effects of washer-bearing-surface size.

Bolt-engagement BC. As shown in Figure 9(c), the spider constraint on the fixture connects the node that represents the bolt end to specified nodes on the inside surface of the threaded insert hole in the fixture thus representing the bolt-engagement BC. In the Baseline-ET model, the entire bottom surface of the hole is used, as shown in Figure 14. Two additional cases (see Figure 14) are also considered: (B1) the spider constraint at the bottom of the hole is maintained, and the ring of nodes at the mid-depth of the hole is used to define an additional spider constraint, and (B2) the spider constraints at the bottom and mid-depth of the hole are maintained, and the ring of nodes at the quarter depth of the hole is used to define an additional spider constraint.

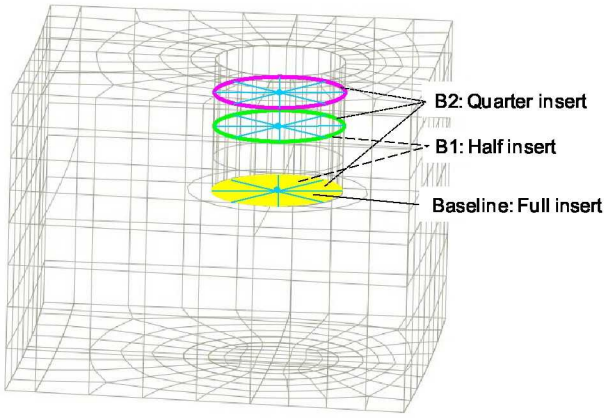

Figure 14. Cases considered to study the effects of bolt-engagement BC.

Coefficient of friction. In the Baseline-ET model, a coefficient of friction of $\mu = 0.1$ is used. Two additional cases are also considered: (F1) $\mu = 0.04$, a general value for the coefficient of friction of Teflon against various materials, and (F2) $\mu = 0.2$.

The results for seal deflection for the parametric studies are compared to the seal deflections from the ET test in Table 2. In Table 2, Δ_z^{test} is the average seal deflection at the target pressure from the ET test, and all the deflections from the analysis predictions are normalized by this value. As expected, the seal deflections increase as the size of the washer bearing surface decreases. For the bolt-engagement BC, the additional spider constraints in cases B1 and B2 effectively shorten the bolt, and it is expected that the seal deflections would decrease. However, the results in Table 2 indicate that the seal deflection increases as the bolt is shortened. This result is not intuitive and warrants further study. Of the three parameters studied, the washer-bearing-surface size has the greatest effect on Δ_z (which is consistent with results reported by Knight, et al. (2008)). The predicted value of Δ_z for case W1 is two percent

Table 2. Seal deflections at the target pressure.

	ET Test Result	ET BOSOR5 Prediction	ET ABAQUS Prediction	
			Parametric Study	Prediction
$\frac{\Delta_z}{\Delta_z^{test}}$	1.0	0.81	Baseline-ET	0.88
			W1	0.98
			W2	1.15
			B1	0.91
			B2	0.93
			F1	0.88
			F2	0.89
			W1 + B1	1.02

different from the test result. The assumed bolt-engagement BC has a lesser effect on Δ_z, and the assumed coefficient of friction has a negligible effect on Δ_z.

One final case is considered that combines cases W1 and B1; i.e., one ring of elements on the MHC is used for the size of the washer bearing surface, and two spider constraints, one at the bottom and one at the mid-depth of the threaded insert hole are used for the bolt-engagement BC. The seal deflection for this case is also presented in Table 2 and is less than two percent different from the test result.

For comparison, the BOSOR5 analysis of seal deflection in the ET test was only within 19 percent of the test result (see Table 2). The ABAQUS analytical configuration that combines cases W1 and B1 correlates most closely with, and conservatively over-predicts, the test result and hence will be used as the modeling practice for all subsequent analyses of the Ares-I US LH2 tank MHC seal joint.

2. Ares-I US LH2 Tank MHC Seal Joint Analyses

Through testing, the ET Project derived their own seal deflection allowable Δ_{ET} for evaluating analysis results. To minimize developmental testing, the US Project has decided to revert back to the original seal deflection specification. Therefore, in this paper, the seal deflections predicted for US are evaluated against the stricter design specification for seal deflection Δ_{spec}. The normalized seal deflections, (Δ_z/Δ_{spec}), are reported. If (Δ_z/Δ_{spec}) is less than unity, then the integrity of the seal is successfully maintained. If (Δ_z/Δ_{spec}) is less than 0.5, then the seal deflection also satisfies the design specification with the one-sided interpretation.

a. Finite Element Model

The forward portion of the Ares-I LH2 tank is shown in Figure 15. The Naflex seal sits between the MHC and the dome-cover flange. The dome-cover flange is welded to the tank dome. The dome is connected to the tank barrel at the Y-ring. The Y-ring is assumed to be rigid.

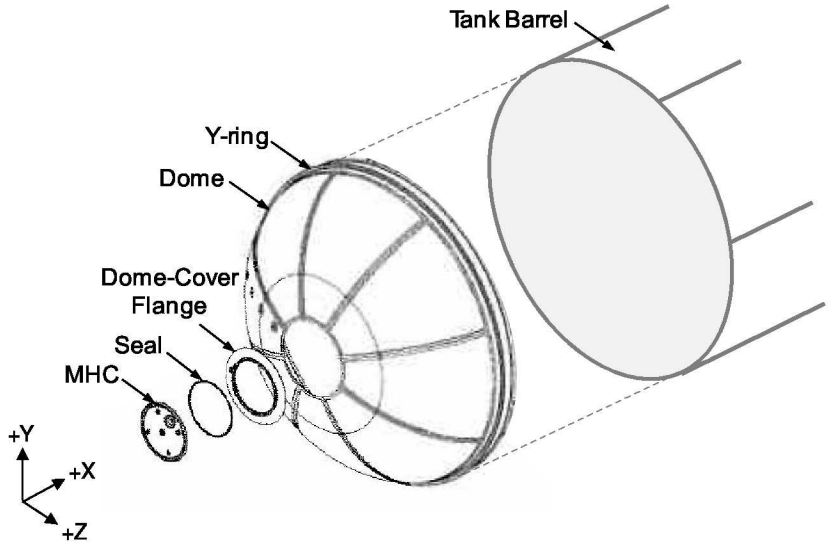

Figure 15. Forward portion of Ares-I US LH2 tank.

The MHC is shown in Figure 16. Most of the acreage of the MHC is a thin shell. To simplify the analyses, the thick regions at penetration bosses shown in the figure are ignored so that symmetry can be exploited. A wedge section of the MHC that encompasses a single bolt hole, or 3.913°, as shown in Figure 16, is used to construct the 3D FE model of the MHC. To construct the model of the Ares-I US LH2 tank MHC seal joint, similar 3.913° portions of the seal, dome-cover flange, and dome are also used, and the modeling characteristics used for the ET test set-up analyses are employed.

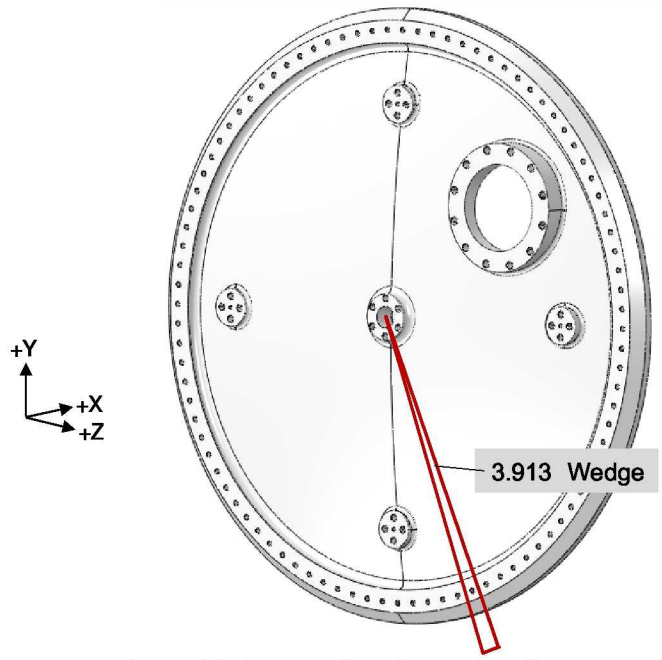

Figure 16. Ares-I US LH2 tank MHC.

The 3D symmetric wedge FE model for the Ares-I US LH2 tank MHC seal joint is presented in Figures 17-21. The model for the entire seal joint assembly is shown in Figure 17. Note the locations of the Y-ring, the seal joint, and the tank axis. The model for the MHC is shown in Figure 18. The model for the seal is the same model used for the ET analyses and is shown in Figure 7. The model for the dome-cover flange is shown in Figure 19, and the model for the dome is shown in Figure 20. The dome-cover flange and dome are connected using a mesh tie constraint to simulate the weld. A mesh tie constraint for shell elements couples all six degrees of freedom between nodes. Along the tied edge, the mesh on the dome has the same refinement as the mesh on the dome-cover flange, resulting in a one-to-one nodal correspondence for the tie constraint. The entire model contains approximately 22000 elements, including 21346 brick elements, 842 shell elements, and 10 beam elements.

Linear, elastic material properties are assumed for all of the materials. The materials used for the current analyses are provided in Table 3.

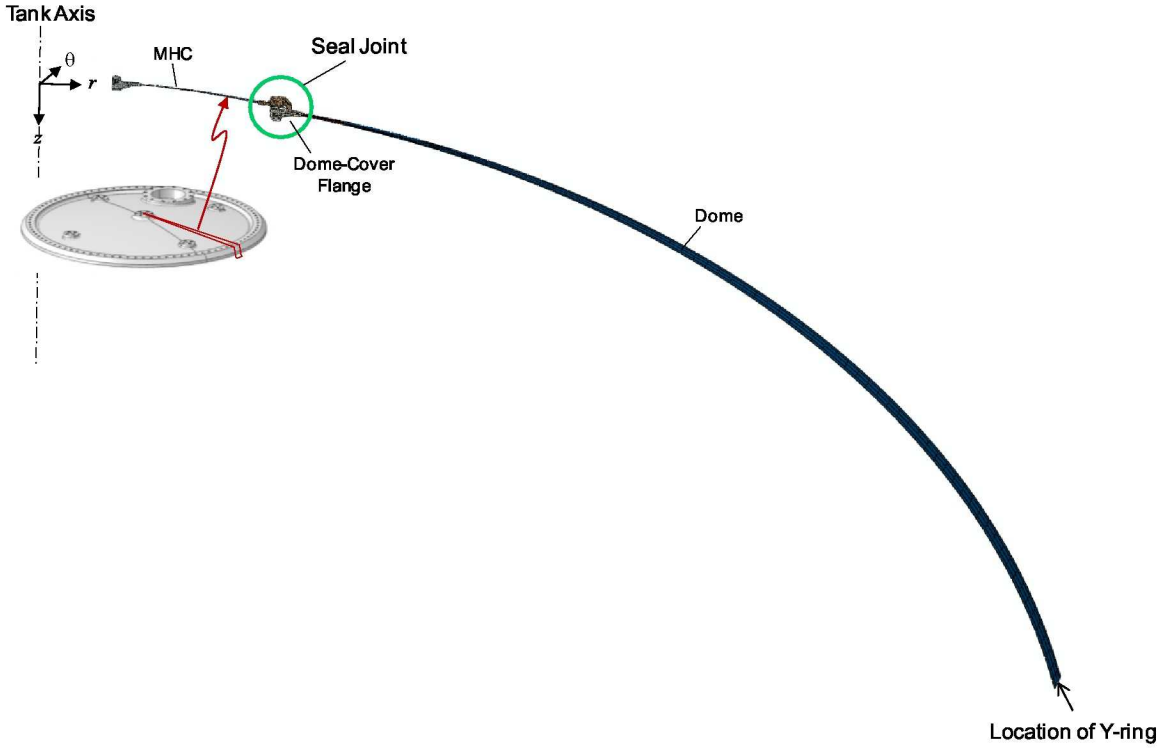

Figure 17. 3D symmetric wedge finite element model of the Ares-I US LH2 tank MHC seal joint.

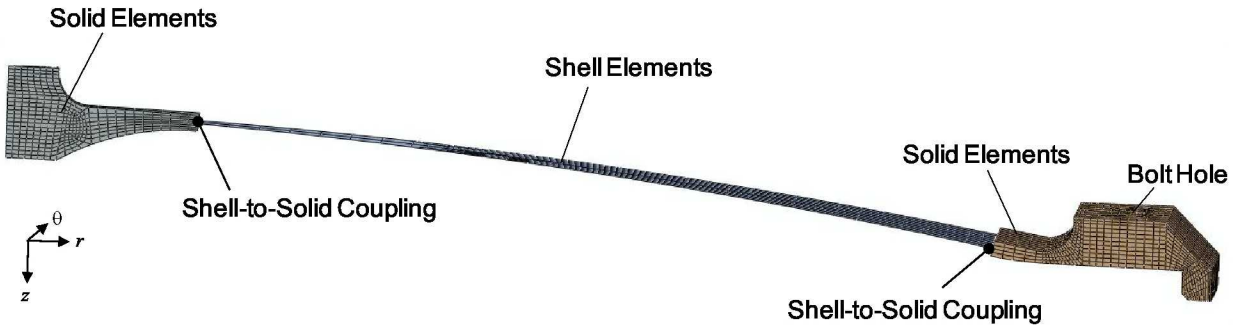

Figure 18. 3D symmetric wedge finite element model of the Ares-I US LH2 tank MHC.

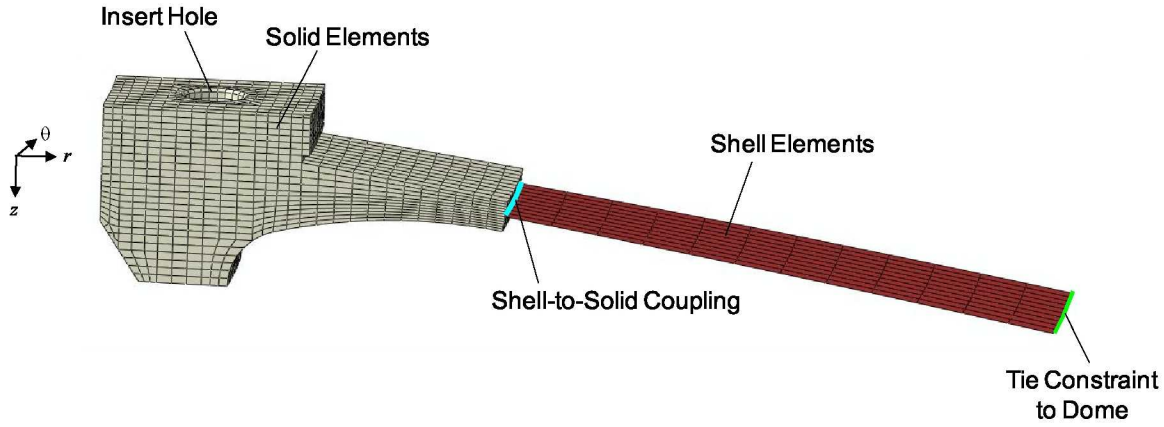

Figure 19. 3D symmetric wedge finite element model of the Ares-I US LH2 tank dome-cover flange.

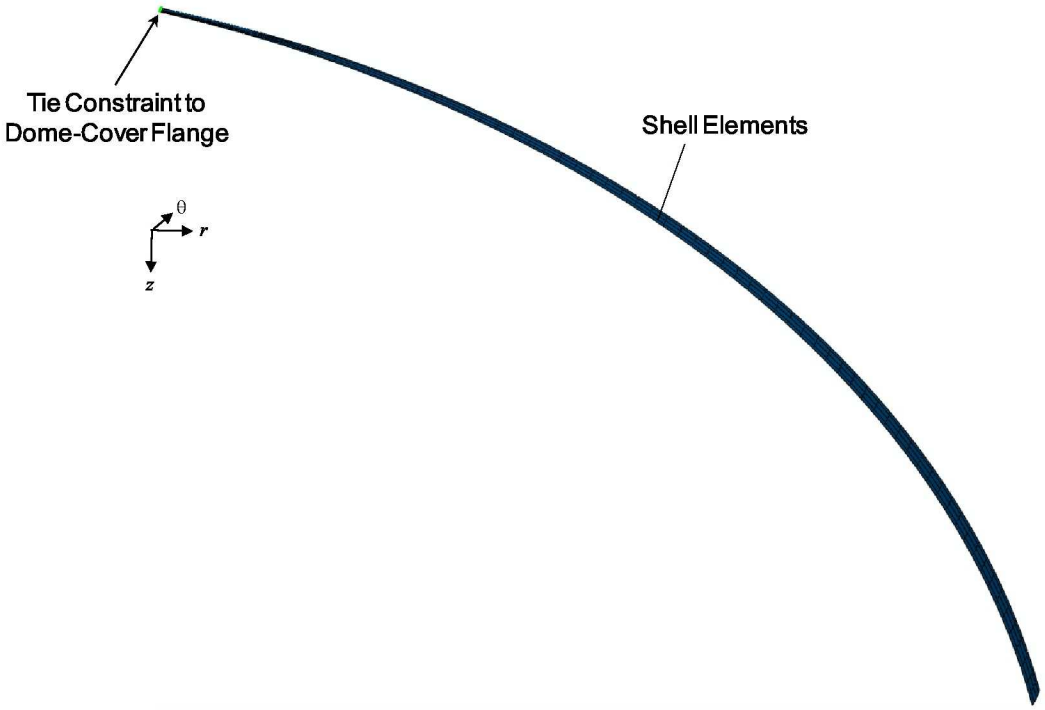

Figure 20. 3D symmetric wedge finite element model of the Ares-I US LH2 tank dome.

Table 3. Linear, elastic material properties for the Ares-I US LH2 tank MHC seal joint analyses.

Part	Material	E, psi @ RT	ν @ RT
MHC, Dome-Cover Flange, Dome	Aluminum 2195	10.7×10^6	0.33
Seal	Inconel 718	30×10^6	0.3
Bolt	A286 Stainless Steel	30×10^6	0.29

The boundary conditions and applied loads are shown in Figure 21. The symmetric boundary conditions and contact definitions from the ET test set-up analyses are also used here. In addition, to simulate the rigid the Y-ring, a fixed boundary condition (i.e., $u_r = u_\theta = u_z = \theta_r = \theta_\theta = \theta_z = 0$) is applied to the bottom of the dome. The bolts are assumed to be 180 ksi A286 fasteners, and the preload is taken to be 65% of the allowable yield stress of the bolt. The pressure load is applied along the entire inside surface of the assembly and around the pressure side of the seal legs as indicated in the Figure 21 insets. The pressure load is 1.4 times the expected flight pressure to account for the joint-separation factor of safety requirement for US. Because there is a hole in the center of the MHC (see Figure 16) where a pressure system component is mounted, there is a thrust load associated with the pressure load. In this paper, the thrust load is assumed to be small because the diameter of the hole in the center of the MHC is small in comparison to the diameter of the MHC ($D_{hole}/D_{MHC} < 0.04$). Therefore, in this paper, the thrust load is not included.

The bolted connection is modeled with three spider constraints as established by the ET test set-up analyses. As such, for the bolt-to-MHC connection, one ring of elements around the bolt hole is used to represent the assumed bearing size of the washer even though the physical diameter of the washer is larger. In addition, for the bolt-to-dome-cover-flange connection, two spider constraints, one using the entire bottom surface of the insert hole and one using the ring of nodes at the insert mid-depth, are used to represent the bolt-engagement BC.

The model described in this section will be referred to as the Baseline-US model.

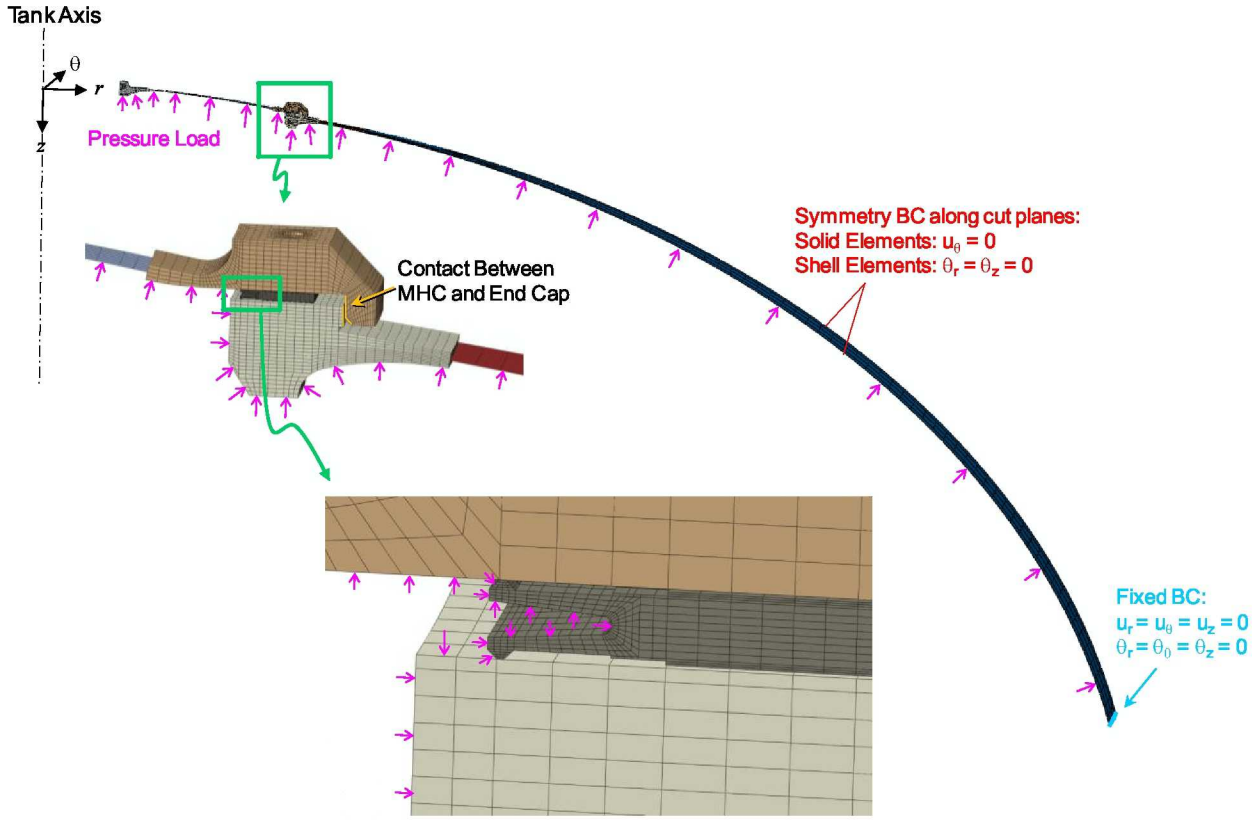

Figure 21. Boundary conditions and load applied to the 3D symmetric wedge finite element model of the Ares-I US LH2 tank MHC seal joint assembly.

b. Results

The u_z displacements for the Baseline-US model subjected to 1.4 times the flight pressure are compared to the original unloaded configuration in Figure 22. (The FE discretization is excluded for clarity.) Because the dome is included in the model, the entire seal joint displaces, especially in the z direction. A close-up of the displacements at the seal primary sealing surface is shown in Figure 23(b). The predicted average seal deflection Δ_z (see Equation 1) for this model is $(\Delta_z / \Delta_{spec}) = 0.39$. This seal deflection is within the design specification with the one-sided interpretation.

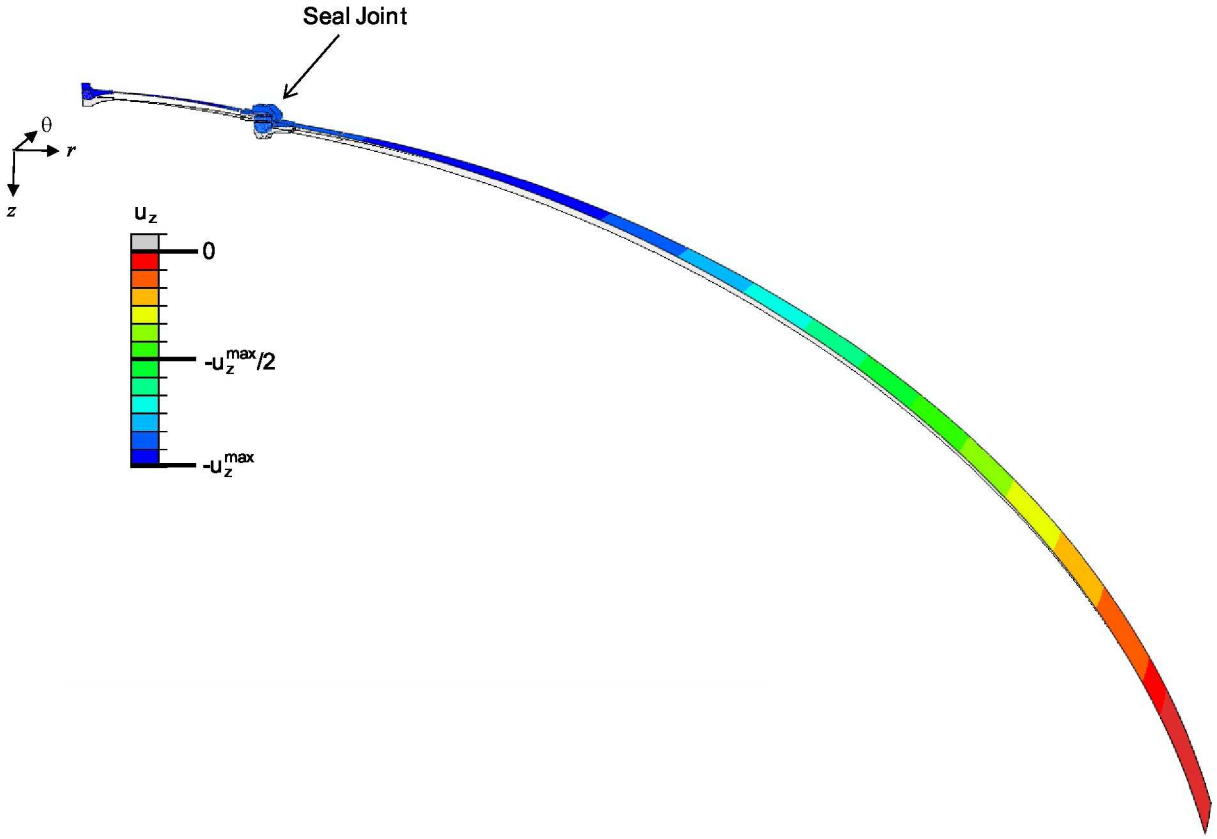

Figure 22. u_z displacements for the Baseline-US model subjected to 1.4 times the flight pressure.

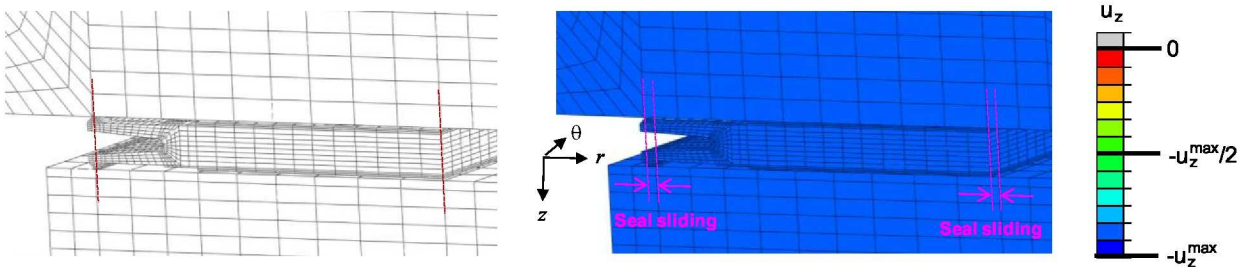

(a) Original configuration (b) u_z displacements

Figure 23. Close-up of u_z displacements at the seal primary sealing surface for the Baseline-US model subjected to 1.4 times the flight pressure.

The tank dome deforms axially and radially due to the pressure load. The MHC is free to move with the dome since, in the Baseline-US model, the MHC is restrained only by the symmetry boundary condition, the spider constraint that simulates the bolt, and the contact with the seal. In the assembled US, a pressurization system component would be bolted to the boss at the center of the MHC. This component is not represented in Baseline-US model. To represent the additional stiffness provided by this component, an additional radial BC is considered, as shown in Figure 24. The nodes along the inner diameter of the MHC are restrained in the r direction (i.e., $u_r = 0$). The results for this case are identical to the results for the Baseline-US model.

Figure 24. Radial restraint at the MHC center.

Again, in the Baseline-US model, the MHC is restrained only through the spider constraint and the contact with the seal, and the dome deforms due to the pressure load. Because of the freedom of movement resulting from this configuration, the seal slides considerably from its original position, as shown in Figure 23. This is in contrast to the ET test set-up model, in which the seal does not slide. For this reason, even though the results from the ET test set-up model indicate that the effects of coefficient of friction are negligible, the study is revisited here. Two cases are considered: $\mu = 0.04$, a general value for the coefficient of friction of Teflon against various materials, and $\mu = 0.2$. The results for the predicted average seal deflection for each of the cases considered are $(\Delta_z / \Delta_{spec}) = 0.39$ and $(\Delta_z / \Delta_{spec}) = 0.38$ for $\mu = 0.04$ and $\mu = 0.2$, respectively. These results are nearly identical to the results for the Baseline-US model. The assumed coefficient of friction has a negligible effect on predicted seal deflection.

c. Cryogenic Temperatures

Cryogenic temperatures are considered since differences in the coefficients of thermal expansion (CTEs) for the joint materials can relieve the initial preload, resulting in greater seal deflection.

The analysis is performed using the Baseline-US configuration and in three solution steps. In the first step, the bolt preload is applied. In the second step, the cryogenic temperature of -423°F is applied to the entire model. In the third step, the pressure load is applied.

An "at-temperature"-type analyses is performed. In at-temperature analyses, the material properties at the final temperature are used for the entire solution sequence (i.e., the material properties are not temperature-dependent). The material properties at cryogenic temperature used for this analysis are provided in Table 4.

Table 4. Linear, elastic material properties at cryogenic temperature.

Part	Material	E_{cryo}, psi	ν_{cryo}	α_{cryo}, in/in/°F
MHC, Dome-Cover Flange, Dome	Aluminum 2195	11.9×10^6	0.33	8.8×10^{-6}
Seal	Inconel 718	31.8×10^6	0.25	5×10^{-6}
Bolt	A286 Stainless Steel	30×10^6	0.29	5.8×10^{-6}

For the Baseline-US model, the bolt preload is based on the allowable yield stress of the bolt. For the cryogenic analysis, the load in the bolt decreases during the analysis due to the application of the temperature. The predicted average seal deflection is $(\Delta_z / \Delta_{spec}) = 0.28$, which is less than the $(\Delta_z / \Delta_{spec})$ due to the same pressure for the Baseline-US analysis at room temperature (i.e., 0.39).

Even though the preload decreases, the seal deflection decreases (in comparison to the Baseline-US model), which is an unexpected result. Subsequent analyses showed that this result is due to two factors. First, the increased stiffness of the materials at cryogenic temperature makes the individual seal joint components stiffer and more capable of resisting deformation. Second, the difference in the CTEs between the aluminum and Inconel causes the

MHC and dome-cover flange to compress against the seal primary sealing surface even further when the temperature is applied. Apparently, the effects of the reduction in bolt preload due to the cryogenic temperature are overcome by the response of the other components of the seal joint (the MHC, seal, and dome-cover flange) to the temperature. However, the result is still not intuitive and will be studied further. With the current results, the predicted seal deflection for the MHC seal joint assembly with cryogenic temperature is within the design specification with the one-sided interpretation.

IV. Concluding Remarks

Analyses of the Ares-I Upper Stage (US) liquid hydrogen (LH2) tank manhole cover seal joint were performed to assess the feasibility that the Naflex seal design used with the Space Shuttle External Tank (ET) manhole covers can successfully be used for the US manhole cover design. The analysis results for the average seal deflections were compared to the US Project design specification limit for seal deflection. The US analyses were performed at 1.4 times the expected flight pressure to comply with the Constellation Program factor of safety requirement on joint separation. The seal deflections for all models considered are within the design specification; therefore, the US manhole cover design using the Naflex seal should perform adequately.

All of the analyses in this paper are three-dimensional symmetric wedge finite element analyses performed using the ABAQUS commercial finite element software. The analysis technique was validated by first modeling a heritage ET seal development leak test and correlating the analysis results for seal deflection to the test results. The modeling practices established using this ET model were used to construct the finite element models for the US analyses.

Results from parametric studies performed with the ET models and the US models demonstrate the effects of several modeling assumptions on the average seal deflection. The assumed size of the washer bearing surface significantly affects the seal deflection, and the bolt-engagement boundary condition affects the seal deflection to a lesser extent. The assumed coefficient of friction for the contact definition has negligible effect on the seal deflection.

The analyses described in this paper have established modeling practices that can be used for future analyses of the Naflex seals in other Ares-I US joint configurations. In these future analyses, the effects of preload and additional loading conditions on seal performance can be further evaluated. The use of commercial analysis software offers a great deal of flexibility both in modeling and interrogation of the results in comparison to the heritage axisymmetric modeling technique employed by the ET Project.

References

Anon. (undated): "Static Cryogenic Seals for Launch Vehicle Applications," NASA Preferred Reliability Practice No. PD-ED-1208.

Anon. (1976): "Seal, Flange, Metallic, 55L6 Qualification Requirements," Product Specification QL55-3, Martin Marietta Michoud Operations, July 16, 1976.

Anon. (ca.2000): "Naflex Cryogenic and High-Temperature Static Face Seals by Langley," Product brochure by Magellan Aerospace Turbine Services, LLC.

Anon. (2001): *Space Shuttle External Tank Critical Items List (CIL)*, Doc. No. MMC-ET-RA04b-K, Lockheed Martin Michoud Space Systems.

Anon. (2008): *Constellation Program Structural Design and Verification Requirements*, NASA CxP 70135, August 25, 2008.

Anon. (2009): *$%$486□$QDO\VLV□8VHU¶V□0DQXDO□±□9ROXPH□,,*, Dassault Systèmes Simulia Corp., Providence, RI.

Bushnell, D. (1974): *BOSOR5 ± A Computer Program for Buckling of Elastic-Plastic Complex Shells of Revolution Including /DUJH□'HIOHFWLRQV□DQG□&UHHS□□9RO□□,□□8VHU¶V□0DQXDO*, Lockheed Missiles & Space Company Report LMSC-D407166, December 1974.

Bushnell, D. (1976): "Buckling of Elastic-Plastic Shells of Revolution with Discrete Elastic-Plastic Ring Stiffeners," *International Journal of Solids and Structures*, Vol. 12, pp. 51-66.

Gillespie, S. E. (1988): *Manhole NAFLEX Seal Leakage Test*, Martin Marietta Manned Space Systems Test Report 826-2369, September 1988.

Knight, N. F., Phillips, D. R., and Raju, I. S. (2008): "Simulating the Structural Response of a Preloaded Bolted Joint," Proceedings of the 49th AIAA SDM Conference, Shaumburg, Illinois, April 7-10, 2008, Paper No. AIAA-2008-1842.

Pilet, J. and Geiman, W. (1997): Space *Shuttle External Tank Stress Analysis*, Lockheed Martin Report MMC-ET-SE05-439, December 1997.

Robbins, R. F. and Ludtke, P. R. (1964): "Review of Static Seals for Cryogenic Systems," *Journal of Spacecraft*, Vol. 1, No. 3, May-June 1964.